

Print Quality Optimization of an Open-Source High-Temperature FDM 3D Printer for Thermoplastic Materials

Evan C. Garrison* and Luke C. Salisbury†
Mississippi State University, Mississippi State, MS, 39762

This paper discusses the optimization of a high-temperature FDM 3D printer tailored specifically for printing polyetheretherketone (PEEK) and polyetherimide (ULTEM/PEI) materials to be released open-source to the public. These materials hold immense promise for applications in medical implants and aerospace systems. However, existing printers designed for processing these materials are cost-prohibitive costs, limiting their use in academia. The printer outlined in this paper is designed to expand the ability for cost-effective research on the materials. The printer employs readily available materials and open-source software to increase access to these materials within academia. This paper will discuss and analyze optimizing the print quality of high-temperature polymers. This paper will further discuss the changes to the mechanical and thermal systems to optimize print quality along with analyzing the effects of differing print parameters on print quality. Based on these results, this paper aims to further optimize this open-source printer design for high-temperature polymers to further the knowledge base within academia.

I. Introduction

ADDITIONAL manufacturing techniques have grown in popularity in recent years and their applications with them. Fused Deposition Modeling (FDM) is one such technique. FDM printers typically use thermoplastic filaments as their feedstock material, which is pushed through a heated nozzle to construct a 3D object one layer at a time[1]. Common filaments that are accessible and easily processed because of their low glass transition temperature include polylactic acid (PLA), polyethylene terephthalate glycol (PETG), and acrylonitrile styrene (ABS)[2]. These low glass transition temperatures do limit the applications of these materials, so they are mostly used for rapid prototyping of parts and low-cost pieces for various non-load-bearing systems[3].

With FDM growing in popularity, the use of high-performance thermoplastic filaments, such as polyetheretherketone (PEEK) and polyetherimide (PEI or ULTEM), has been explored in recent years. With higher glass transition rates, more robust heating systems are required, especially as it concerns the hot end[4]. Higher bed temperatures and ambient chamber temperatures are also necessary[5]. However, these material properties also make the filaments promising for use in medical implants[6] and aerospace systems[5].

Currently, commercially available printers are cost-prohibitive and lacking modularity which has led to little research conducted on the materials, especially in academia. The price of high-temperature 3D printers on the market range from 2,500 dollars to well over 50,000 dollars. The cheaper options have small build volumes and yield low-quality parts. Commercial printers are also not modular, preventing the adjustment of various print parameters to identify their relationship with print quality and mechanical properties.[7].

Previously, an open-source high-temperature FDM 3D printer was developed to investigate these relationships and to expand the knowledge base regarding and access to high-performance thermoplastics in academia[7]. This printer was unable to print quality parts out of high-performance materials in its initial configuration. Bed adhesion frequently did not occur, leading to wasted prints. Even when it did occur, high levels of warping and layer shifting were present, leading to low-quality prints or otherwise preventing completion of the part. This paper seeks to address these print quality issues by optimizing the printer's mechanical systems, thermal systems, and print parameters.

*Undergraduate Researcher, Department of Aerospace Engineering, 501 Hardy Road, 321 Walker Hall, Drawer A, Mississippi State, MS 39762, AIAA Student Member.

†Undergraduate Researcher, Michael W. Hall School of Mechanical Engineering, 479-1 Hardy Road, 210 Carpenter Hall, Box 9552, Mississippi State, MS 39762, AIAA Student Member.

II. Methodology

Three areas of optimization were identified to improve print quality; mechanical systems, thermal systems, and print parameters. The experiments carried out sought to address each in turn. Principally, the sources of variation and randomness within the mechanical and thermal systems were identified by visual and physical inspection of the printer. New parts and processes were prototyped to verify their effectiveness. This process was repeated for all areas of concern until the variations were observed to have been minimized and validated by tests of the printer's motion and quality of prints.

The print parameters were then optimized to increase bed adhesion and print quality using a full factorial design of experiment. This was carried out in two parts. The first part sought to identify the hot end and bed temperatures at which part adhesion occurred most often. Five levels were tested for bed temperatures, starting at 120°C and increasing in increments of 10, with a maximum temperature of 160°C tested. Three levels of hot end temperatures were tested, starting at 370°C and increasing in increments of 10, with a maximum temperature of 390°C. This resulted in 15 total experiment groups. For each group, three tests were run and adhesion was rated on a scale of 0-3. Zero was defined as no observed adhesion, one as limited observed adhesion, two as observed adhesion that suffered from warping or otherwise broke off, and three as complete adhesion with no visual defects. Data was recorded for all 45 trials and then processed using a MATLAB script that compared the data to a linear model and plotted the data on a three-variable interaction plot to identify the temperatures at which adhesion was feasible.

Temperatures identified as allowing for bed adhesion were tested in combination with the volumetric flow rate in part two of the parameter optimization. Three levels of volumetric flow rate were tested, starting at 15 mm³/s and increasing in increments of 3, with a maximum rate of 21 mm³/s. Three tests were conducted for each group and adhesion was rated on a scale of 0-4. Zero was defined as no observed adhesion, one as partial adhesion but no part formation, two as partial adhesion with part formation, three as full adhesion with warping or shifting before infill, and four as full adhesion with no warping or shifting before infill. Data was recorded for all trials and then processed using a MATLAB script that compared the data to a linear model and plotted the data on a four-variable interaction plot to identify parameters at which bed adhesion and print quality are the highest.

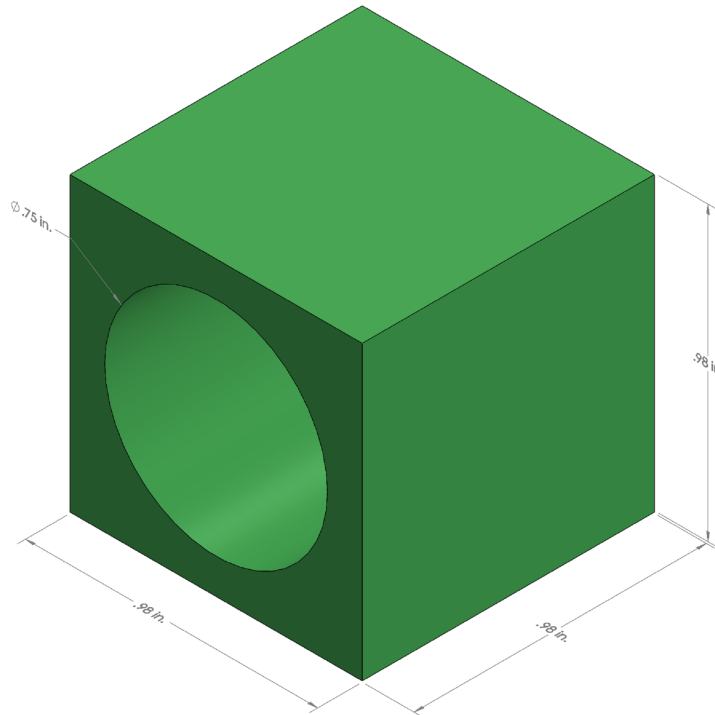


Fig. 1 CAD Model of Test Piece with Dimensions

For all trials, the test piece in Fig. 1 was used. All print parameters not tested by the DOEs were held constant. Notably, the layer height was set to 0.12 mm, extrusion width was set at 0.42 mm, and the ambient chamber temperature was held around 80°C. ULTEM was the filament used for the tests.

III. Mechanical Optimization

Previous parts created using the printer had visible issues with layer shifting. These were persistent issues regardless of the material being printed, the parameters used, or the part's complexity. To mitigate the random variations in print quality and to achieve more consistency, the mechanical systems were visually and physically inspected to identify potential sources of variation.

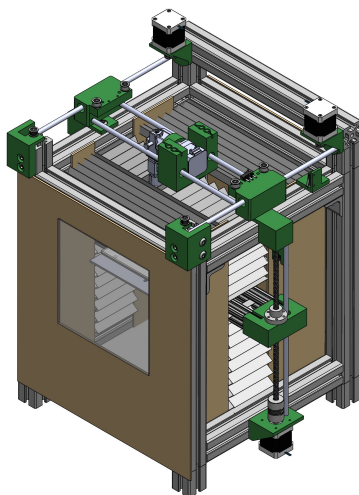


Fig. 2 Original CAD Model of the Printer

Figure 2 displays the initial design and assembly of the printer. The CoreXY system in this iteration was identified as a potential source of discrepancies in print quality. Upon analyzing the mechanical systems of the CoreXY mechanism, it was found that the initial design and construction led to a noticeable oscillation within the extruder carriage which directly led to defects and variance within parts. Another potential cause of print instability identified was the degradation of polyethylene terephthalate glycol (PETG) parts. During the printing process, the material was exposed to stresses at temperatures exceeding the material's glass transition temperature, leading to warping and bowing of all carriage components. The mechanical optimization of the printer was focused on addressing these flaws.

A. Y-Axis Carriages

The locations with the most notable vibrations were in the Y-axis and extruder carriages. In the original design and construction of the printer, only two linear guide rods were utilized for the Y-axis. This meant that each Y-axis carriage was held in place by a single rod located near the top of the part. Initially, no issues were observed. Despite this, the carriage was found to rotate around the stabilization rod over time due to a moment caused by the weight of the X-axis linear rods, extruder, and extruder carriage. This rotation caused the Y-axis carriages to be at an angle below parallel where they attached to the X-axis. This rotation was present on both sides of the printer, making the extruder carriage out of plane with the Y-axis and causing the hot end to vibrate while printing. The weight of the extruder carriage assembly also led to bending in the horizontal stabilization rods, further decreasing the alignment of the system and increasing the vibrations of the print head.

To address these issues, the CoreXY system was redesigned, tested, and optimized to increase its rigidity. Having identified the Y-axis carriages as the greatest source of variance, they were the first parts to be recreated. The new part needed to be prevented from rotating because the moment due to the weight of the X-axis linear rods, extruder, and extruder carriage could not be removed. The design would also need to decrease the load that each stabilization rod bore so that the bending in the Y-axis could be reduced. To do this, two more stabilization rods were added, one on each side. The existing linear rods remained at the top of their respective parts, but the new ones were added at the base of the part. Upon installation of the new carriages, the rotation could no longer be observed and the bending in the linear rods was reduced as the load was distributed across the four rods and the additional rods increased the stability of the carriages.

B. Other Parts

While updating the carriages did increase the alignment of the print head with the X-Y plane, the hot end was still misaligned due to the compensations that had been incorporated in the initial design because of the obvious bending and rotation, specifically in the positioning of the Y-axis motor mounts. These parts were redimensioned and constructed to be positioned accurately in the context of the lack of bending. To promote prolonged alignment and use of the printer, the pulley attachments were also reinforced and realigned for optimized belt placement.

The obvious deformations in the parts could not be connected to specific issues in the performance of the printer. However, to ensure that they would not impact print quality due to worsening conditions in the future, all of the parts were replaced. Most of the parts had initially been printed using PETG. The new parts were printed with acrylonitrile butadiene styrene (ABS). ABS was chosen as the replacement material for all parts as its glass transition temperature is 105°C [8], which is greater than the heater target temperature of 80-90°C. With a higher glass transition temperature, ABS is more resistant to deformations caused by heat and can withstand higher temperatures for greater periods, both of which are necessary when printing at high temperatures and maintaining elevated chamber temperatures. Figure 3 displays all of the changes made to the CoreXY assembly and the top of the printer.

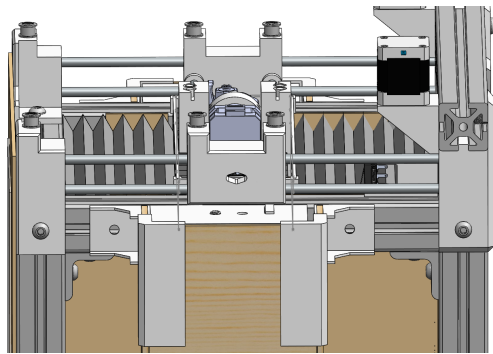


Fig. 3 CAD Model of Optimized CoreXY System

IV. Thermal Optimization

The initial iteration of the heated chamber could not reach and maintain high ambient temperatures for printing high-temperature thermoplastics, such as ULTEM. Results had to be artificially achieved by holding the bed at a higher temperature. Even then print quality was low and the ambient temperature was measured to be around 60°C by a thermocouple in the chamber. Reaching this stabilizing temperature, even though it was low, would take an hour. All of these issues created the need to optimize the thermal systems of the printer, which includes the heater and the chamber.

A. Heater

The chamber of the printer is heated by a 1000-watt ceramic heater. In the initial design, a hole was cut in the bottom of the chamber and insulation in which the unit was placed to allow it to draw in outside air. The heater was created with an internal emergency shut-off that is triggered if the unit reaches 160°C. Even with the heater reaching its maximum temperature, natural convection was insufficient to effectively transfer the heat to the air in the chamber.

To increase the rate of heat transfer, a 120 mm computer fan was placed below the hole and heater and run at its lowest speed setting. The maximum chamber temperature was marginally increased to 80°C, but it was hard to maintain and took nearly two hours to reach a stabilizing temperature. The fan was then moved inside of the chamber but remained below the heater. Insulation strips were used to seal the excess gaps between the fan and the hole and also to protect the fan from direct contact with the unit. The fan was run at its lowest speed and a chamber temperature of 140°C was achieved, though it took an hour and a half to stabilize. Placing the fan inside the chamber was determined to be the optimal way to increase the rate of heat transfer to the air in the chamber. A duct that could safely connect the fan to the heater and seal the gaps between the fan and the hole in the bottom of the chamber was designed and printed out of ABS to replace the strips of insulation.

B. Enclosure

Reaching and maintaining a stabilizing temperature high enough to print ULTEM and PEEK was still not possible in a reasonable timeframe, even with the adjustments to the heater. Once the required temperatures were achieved, an oscillation of 10°C was still observed. Using a thermometer and physical inspection, the largest temperature drops were found to be near the Z-axis and at the top where bellows had initially been used to insulate the chamber. In their initial position, the bellows were incapable of sealing the chamber when collapsed because gaps would form that allowed heat to escape. A more robust insulation technique was necessary to optimize the thermal performance of the chamber.

Previously, the design had to prioritize keeping certain parts out of the chamber because they were made of PETG and would have deformed in the presence of the required ambient temperature. Having replaced these parts with redesigned versions made of ABS, this was no longer a concern. For the holes in the sides of the chamber, this meant the technique used to insulate the rest of the chamber could be utilized. Three wood panels were used on each side to enclose the Z-axis system within the chamber. The panels were covered with mineral wool insulation that was a half inch thick like the rest of the chamber. The mount for the Z-axis linear rods at the top of the printer was expanded to serve as a cap for the side enclosures. The bottom of the side enclosures was left open to allow some air to escape and to prevent the Z-axis stepping motors from overheating.

Enclosing the top of the chamber was a greater challenge, as the extruder has a maximum operating temperature of 80°C [9] and the enclosure must be modular so the CoreXY system can move. The bellows were determined to be the most effective way to do this. Initially, they had been attached near the top of the extruder carriage. This positioning placed the bellows above the plane the top of the printer frame is in. As such, when they collapsed, gaps would form above the printer. To remove these gaps, a new attachment system was designed that allowed the bellows to be connected below the extruder carriage, thereby mitigating the heat it would experience while also removing the gaps from which heat was escaping. Figure 4 depicts the changes made to the thermal systems and is the most up-to-date CAD model of the printer.

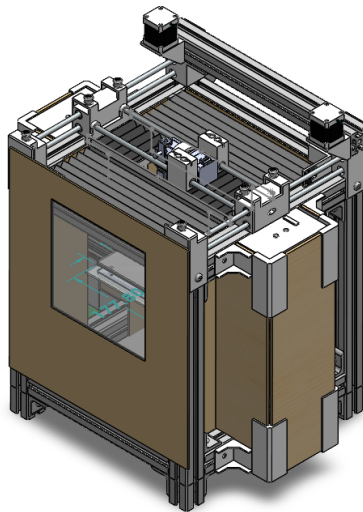


Fig. 4 Optimized CAD Model of the Printer

Having made these adjustments, the stabilizing temperature of the chamber was again tested by letting the heater run freely with the fan on low below it. Now, the chamber reached 160°C in ten minutes. Additionally, fluctuations in the ambient temperature were reduced to 2°C. These adjustments to the chamber optimized its thermal performance, addressing the flaws of the initial design.

C. Temperature Control

For high-temperature polymers like ULTEM and PEEK, chamber temperatures of 70-100°C are all that is necessary, though the higher temperatures obtained will be required to print other materials in the future. For current trials, however, the ambient heat needs to be regulated so that it is not too high. For the trials in this paper, 80°C was the targeted temperature.

The fan below the heater was determined to be an easy way to control the ambient temperature. It was observed that changing the fan speed directly impacted the temperature of the chamber, as higher speeds decreased the temperature in the chamber. Using the control dial, a speed was found that resulted in a measured chamber of 80°C. Even at the lower temperature, fluctuations were observed to be around 2°C. With the ability to control ambient temperature with a high degree of accuracy, the thermal systems were considered to be optimized.

V. Print Parameter Optimization

Throughout testing of the printer, bed adhesion was identified as the largest barrier to successful and quality prints of ULTEM. When first testing the printer with PETG, similar issues had prevented quality prints. For PETG, existing literature and a variety of tests were utilized to identify print parameters at which higher-quality prints could be achieved. Hot end temperature, bed temperature, volumetric flow rate, extrusion width, and print speed were all adjusted. This solved the adhesion issue. The same approach was used in this paper to improve the quality of prints made of ULTEM. The parameters considered are hot end temperature, bed temperature, and volumetric flow rate.

A. Hot End and Bed Temperature

The temperature of the hot end and bed were the first parameters tested. A baseline was set by the temperature ranges at which the manufacturer recommends printing ULTEM. Table 1 displays the parameters tested and values returned by the full factorial design of experiment and adhesion scale.

Table 1 Adhesion Level Resulting From Differing Hot End and Bed Temperatures

Trial Number	Hot End (°C)	Bed (°C)	Level of Adhesion
1	370	120	0
2	370	120	0
3	370	120	0
4	370	130	1
5	370	130	1
6	370	130	1
7	370	140	0
8	370	140	1
9	370	140	1
10	370	150	1
11	370	150	1
12	370	150	0
13	370	160	1
14	370	160	1
15	370	160	1
16	380	120	1
17	380	120	0
18	380	120	1
19	380	130	1
20	380	130	1
21	380	130	1

Trial Number	Hot End (°C)	Bed (°C)	Level of Adhesion
22	380	140	1
23	380	140	2
24	380	140	2
25	380	150	2
26	380	150	2
27	380	150	2
28	380	160	2
29	380	160	2
30	380	160	0
31	390	120	0
32	390	120	0
33	390	120	0
34	390	130	0
35	390	130	1
36	390	130	1
37	390	140	1
38	390	140	1
39	390	140	1
40	390	150	1
41	390	150	1
42	390	150	1
43	390	160	0
44	390	160	1
45	390	160	1

This data was imported into MATLAB and analyzed by a script to identify the impact hot end and bed temperatures have on bed adhesion. The script found p-values of 1 and 0.94995 for the hot end and bed temperatures respectively. Both of these values suggest a statistically significant correlation between the parameter and bed adhesion. The script also generated a three-value interaction plot, displayed in Fig. 5, that shows the relationship between the temperatures of the hot end and bed and the level of adhesion achieved.

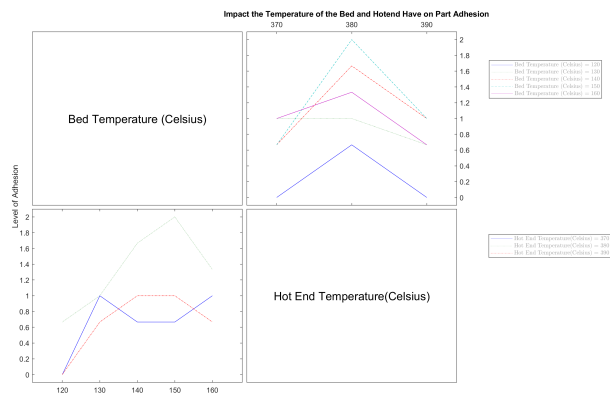


Fig. 5 Interaction Plot for Bed Temperature, Hot End Temperature, and Level of Adhesion

Based on Fig. 5, bed temperatures of 140°C to 160°C were identified as viable for part adhesion as they surpassed a

level of adhesion of 1 for at least one hot end temperature. Figure 5 also suggests all three hot end temperatures tested showed potential for part adhesion, though higher temperatures yielded better results for both the hot end and bed.

B. Hot End Temperature, Bed Temperature, and Volumetric Flow Rate

The results displayed in Table 1 and Fig. 5 were used to establish the levels of the full factorial design of experiment to be tested when also considering the volumetric flow rate. Three levels of hot end temperatures (370°C, 380°C, and 390°C) were used as before. However, bed temperatures were limited to the three levels identified to have potential for adhesion in the previous DOE (140°C, 150°C, and 160°C). When combined with the three levels of volumetric flow rates, this resulted in 27 different experimental groups. Each group was tested three times, creating 81 trials. The second adhesion scale described in the methodology was used for this part of the experiment. Table 2 displays the results.

Table 2 Adhesion Level Resulting From Differing Hot End Temperatures, Bed Temperatures, and Flow Rates

Trial Number	Hot End (°C)	Bed (°C)	Flow Rate (mm ³ /s)	Level of Adhesion
1	370	140	15	0
2	370	140	15	0
3	370	140	15	0
4	370	150	15	0
5	370	150	15	0
6	370	150	15	0
7	370	160	15	1
8	370	160	15	1
9	370	160	15	0
10	380	140	15	0
11	380	140	15	0
12	380	140	15	0
13	380	150	15	0
14	380	150	15	0
15	380	150	15	0
16	380	160	15	0
17	380	160	15	0
18	380	160	15	0
19	390	140	15	0
20	390	140	15	0
21	390	140	15	0
22	390	150	15	0
23	390	150	15	0
24	390	150	15	0
25	390	160	15	1
26	390	160	15	1
27	390	160	15	1
28	370	140	18	0
29	370	140	18	0
30	370	140	18	0
31	370	150	18	0
32	370	150	18	0

Trial Number	Hot End (°C)	Bed (°C)	Flow Rate (mm ³ /s)	Level of Adhesion
33	370	150	18	0
34	370	160	18	1
35	370	160	18	1
36	370	160	18	1
37	380	140	18	1
38	380	140	18	1
39	380	140	18	1
40	380	150	18	1
41	380	150	18	1
42	380	150	18	1
43	380	160	18	2
44	380	160	18	2
45	380	160	18	2
46	390	140	18	2
47	390	140	18	2
48	390	140	18	1
49	390	150	18	3
50	390	150	18	3
51	390	150	18	3
52	390	160	18	3
53	390	160	18	3
54	390	160	18	3
55	370	140	21	1
56	370	140	21	1
57	370	140	21	1
58	370	150	21	1
59	370	150	21	1
60	370	150	21	1
61	370	160	21	1
62	370	160	21	1
63	370	160	21	1
64	380	140	21	2
65	380	140	21	2
66	380	140	21	1
67	380	150	21	2
68	380	150	21	2
69	380	150	21	2
70	380	160	21	2
71	380	160	21	2
72	380	160	21	2
73	390	140	21	1
74	390	140	21	1
75	390	140	21	2
76	390	150	21	2

Trial Number	Hot End (°C)	Bed (°C)	Flow Rate (mm ³ /s)	Level of Adhesion
77	390	150	21	2
78	390	150	21	2
79	390	160	21	2
80	390	160	21	2
81	390	160	21	2

The experimental data was imported into MATLAB and analyzed by a script to identify the impact hot end temperature, bed temperature, and volumetric flow rate have on bed adhesion. The script found p-values that were not statistically significant for any factor, which is contradictory to what the initial DOE found concerning the hot end and bed temperatures. The script generated the interaction plot in Fig. 6 as well.

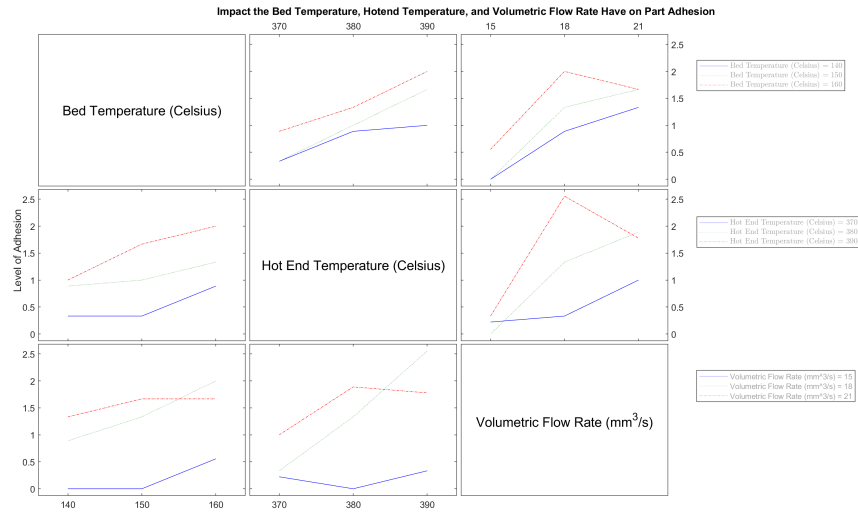


Fig. 6 Interaction Plot for Bed Temperature, Hot End Temperature, Flow Rate, and Level of Adhesion

Figure 6 demonstrates that increasing hot end and bed temperatures led to higher levels of bed adhesion in nearly every case. A higher volumetric flow rate also generally resulted in better bed adhesion, though there are more exceptions to this trend. When looking at Table 2, these trends appear to persist through the vast majority of the 81 trials.

VI. Discussion and Conclusion

Optimization of the printer was successful in achieving better print quality. The mechanical optimization of the printer led to a greater degree of consistency in the positioning of the printer head and mitigated the vibrations that had been observed. Through these improvements, parts can be constructed more accurately. The largest impact of the mechanical optimization was observed in the reduction of layer shifting. With consistent layering, higher quality parts can be created with greater dimensional accuracy. The positioning of the Z-axis was not addressed by the mechanical optimization this paper discusses. When conducting test prints, it was observed that the current microstep of the motors in the Z-direction is too large. This leads to the printer head being too far from the build surface allowing for greater discrepancies in the flow of the filament. Future investigation could be conducted into replacing the stepping motors with more accurate ones to see if this promotes greater consistency in the movement of the filament from the hot end to the build.

The thermal optimization of the printer led to ambient heat with greater maximum temperatures, fewer fluctuations in heat, and a higher degree of control over the chamber temperature. When extruding and printing ULTEM, a more consistent flow of filament was observed. The material had fewer bubbles and did not cool before reaching the bed as often. The impact of ambient heat on print quality was not examined and should be investigated in the future as it could allow for lower hot end and bed temperatures. Additionally, the distribution of the ambient heat was not analyzed.

Larger and longer prints than were conducted for this paper will require an even distribution of heat. Analysis will need to be conducted to determine the current distribution of heat and to find ways to optimize it.

Optimization of the print parameters had the most notable impact on print quality, yielding the highest levels of adhesion. Generally, higher print and bed temperatures generated higher quality parts. Changing the chamber temperature in the future could alter these results. Higher volumetric flow rates also lead to better prints, despite the lack of a statistically significant relationship. This is likely due to the aforementioned lack of accuracy in the microstep. Because of the increased amounts of filament being extruded for each layer, the print head needed to be moved away from the build. Doing so created a gap that was too large and where the filament was observed to cool and begin warping before contacting the bed. Higher ambient temperatures or a more accurate microstep could address this issue. Additionally, other parameters could be tested to determine their impact and to address the issues that higher volumetric flow rates experienced. A higher extrusion width specifically could help to mitigate the flaws observed.

Print quality was improved by the optimizations performed in this test and print parameters that tend to yield better parts were identified. This research creates a basis by which the open-source printer can be refined so that it can create builds comparable to commercial printers. Expanding access to high performance thermoplastics in academia via this printer could yield significant benefits in aerospace and biomedical fields. Further research is necessary into the performance of the materials, especially PEEK, for these benefits to be realized. This optimized open-source high-temperature printer expands the existing knowledge base, creating opportunities for these future investigations.

Acknowledgments

We would like to thank the Bagley College of Engineering and Michael W. Hall School of Mechanical Engineering for their generous financial support that enabled this research. We would also like to thank Dr. Matthew W. Priddy of the Michael W. Hall School of Mechanical Engineering and Dr. Santanu Kundu of the Dave C. Swalm School of Chemical Engineering for their support, guidance, mentorship, and provision of laboratory spaces and resources. Finally, we would like to thank Charlotte Thompson for getting this project off the ground and for continually offering support, advice, and mentorship for all of our research endeavors. Our research would not have been possible without these supporters.

References

- [1] Carolo, L., "What Is FDM 3D Printing? – Simply Explained," 2024. URL <https://all3dp.com/2/fused-deposition-modeling-fdm-3d-printing-simply-explained/>, accessed: 02-03-2025.
- [2] Bates-Green, K., and Howie, T., "Materials for 3D Printing by Fused Deposition," *Technician Education in Additive Manufacturing and Materials*, 2017. URL https://www.materialseducation.org/educators/matedu-modules/docs/Materials_in_FDM.pdf.
- [3] Das, A., Chatham, C., Fallon, J., Zawaski, C., Glimer, E., Williams, C., and Bortner, M., "Current understanding and challenges in high temperature additive manufacturing of engineering thermoplastic polymers," *Additive Manufacturing*, Vol. 34, 2020. <https://doi.org/https://doi.org/10.1016/j.addma.2020.101218>.
- [4] Ding, S., Zhou, B., Wang, P., and Ding, H., "Effects of nozzle temperature and building orientation on mechanical properties and microstructure of PEEK and PEI printed by 3D-FDM," *Polymer Testing*, Vol. 78, 2019. <https://doi.org/https://doi.org/10.1016/j.polymertesting.2019.105948>.
- [5] Boytsov, E. A., Blaginin, S., and Sinkov, A., "Why we Need a Heated Chamber for 3D Printing with 'High Performance' Polymers?" *Modern Trends in Manufacturing Technologies and Equipment*, 2021. URL <https://api.semanticscholar.org/CorpusID:251392276>.
- [6] Wang, Y., Müller, W.-D., Rumjahn, A., Schmidt, F., and Schwitalla, A. D., "Mechanical properties of fused filament fabricated PEEK for biomedical applications depending on additive manufacturing parameters," *Journal of the Mechanical Behavior of Biomedical Materials*, Vol. 115, 2020. <https://doi.org/https://doi.org/10.1016/j.jmbbm.2020.104250>.
- [7] Thompson, C., "Design and Construction of an Open-Source High-Temperature FDM 3D Printer for Thermoplastic Materials," 2025. Unpublished.
- [8] Polymaker, "PolyLite™ ABS Technical Data Sheet," No Date. URL https://cdn.shopify.com/s/files/1/0548/7299/7945/files/PolyLite_ABS_TDS_EN_V5.4.pdf?v=1731955200, accessed: 02-03-2025.
- [9] Bondtech, "Bondtech QR Extruder Technical Data Sheet," No Date. URL <https://cdn.shopify.com/s/files/1/0252/5285/5880/files/QR-3.0.pdf?v=1622639704>, accessed: 02-03-2025.